

Measurement of the relative neutron sensitivity curve of a $LaBr_3$(Ce) scintillator based on the CSNS Back-n white neutron source

Jian Liu(刘建), Dongming Wang(王东明), Yuecheng Fu(甫跃成), Zhongbao Li(李忠宝), Han Yi(易晗), and Longtao Yi(易龙涛)

Citation: Chin. Phys. B, 2023, 32 (**10**): 100703. DOI: 10.1088/1674-1056/acca08
Journal homepage: http://cpb.iphy.ac.cn; http://iopscience.iop.org/cpb

What follows is a list of articles you may be interested in

Direct measurement of an energy-dependent single-event-upset cross-section with time-of-flight method at CSNS

Biao Pei(裴标), Zhixin Tan(谭志新), Yongning He(贺永宁), Xiaolong Zhao(赵小龙), and Ruirui Fan(樊瑞睿)
Chin. Phys. B, 2023, 32 (**2**): 020705. DOI: 10.1088/1674-1056/aca603

X-ray focusing using an x-ray lens composed of multi-square polycapillary slices

Kai Pan(潘凯), Tian-Cheng Yi(易天成), Zhao Wang(王婴), Mo Zhou(周末), Yu-De Li(李玉德), Zhi-Guo Liu(刘志国), Xiao-Yan Lin(林晓燕), and Tian-Xi Sun(孙天希)
Chin. Phys. B, 2022, 31 (**2**): 020701. DOI: 10.1088/1674-1056/ac381a

Study on γ-ray source from the resonant reaction $^{19}F(p,\alpha\gamma)^{16}O$ at E_p=340 keV

Fu-Long Liu(刘伏龙), Wan-Sha Yang(杨婉莎), Ji-Hong Wei(魏继红), Di Wu(吴笛), Yang-Fan He(何阳帆), Yu-Chen Li(李雨尘), Tian-Li Ma(马田丽), Yang-Ping Shen(谌阳平), Qi-Wen Fan(樊启文), Chuang-Ye He(贺创业), Bing Guo(郭冰), Nai-Yan Wang(王乃彦)
Chin. Phys. B, 2020, 29 (**7**): 070702. DOI: 10.1088/1674-1056/ab96a0

Photo-transmutation based on resonance γ-ray source

Guang-Yong Fu(付光永), Yong-Le Dang(党永乐), Fu-Long Liu(刘伏龙), Di Wu(吴笛), Chuang-Ye He(贺创业), Nai-Yan Wang(王乃彦)
Chin. Phys. B, 2019, 28 (**6**): 060707. DOI: 10.1088/1674-1056/28/6/060707

New measurement of thick target yield for narrow resonance at E_x=9.17 MeV in the $^{13}C(p,\gamma)^{14}N$ reaction

Yong-Le Dang(党永乐), Fu-Long Liu(刘伏龙), Guang-Yong Fu(付光永), Di Wu(吴笛), Chuang-Ye He(贺创业), Bing Guo(郭冰), Nai-Yan Wang(王乃彦)
Chin. Phys. B, 2019, 28 (**6**): 060706. DOI: 10.1088/1674-1056/28/6/060706

INSTRUMENTATION AND MEASUREMENT

Measurement of the relative neutron sensitivity curve of a $LaBr_3$(Ce) scintillator based on the CSNS Back-n white neutron source

Jian Liu(刘建)[1], Dongming Wang(王东明)[1], Yuecheng Fu(甫跃成)[1], Zhongbao Li(李忠宝)[1], Han Yi(易晗)[2], and Longtao Yi(易龙涛)[1,†]

[1] *Institute of Nuclear Physics and Chemistry, China Academy of Engineering Physics, Mianyang* 621900, *China*
[2] *Spallation Neutron Source Science Center, Dongguan* 523803, *China*

(Received 30 October 2022; revised manuscript received 31 March 2023; accepted manuscript online 4 April 2023)

A scintillator detector consisting of a $LaBr_3$(Ce) (0.5%) scintillator, a photomultiplier tube (PMT), and an oscilloscope were used to study the neutron sensitivities of the $LaBr_3$(Ce) scintillator at the China Spallation Neutron Source (CSNS) Back-n white neutron source in the double-bunch and single-bunch operation modes, respectively. Under the two operational modes, the relative neutron sensitivity curves of the $LaBr_3$(Ce) scintillator in the energy regions of 1–20 MeV and 0.5–20 MeV were obtained for the first time. In the energy range of 1–20 MeV, the two curves were nearly identical. However the relative neutron sensitivity uncertainties of the double-bunch experiment were higher than those of the single-bunch experiment. The above results indicated that the single-bunch experiment's neutron sensitivity curve has a lower minimum measurable energy than the double-bunch experiment. Above the minimum measurable energy of the double-bunch experiment, there is little difference between the measured relative neutron sensitivity curves of the single-bunch and double-bunch experiments of the $LaBr_3$(Ce) scintillator and those of other scintillators with a similar neutron response signal intensity.

Keywords: relative neutron sensitivity, $LaBr_3$(Ce), China Spallation Neutron Source (CSNS), white neutron source

PACS: 07.85.Fv, 29.40.Mc, 78.70.Ps, 29.40.–n **DOI:** 10.1088/1674-1056/acca08

1. Introduction

The absolute measurement of gamma radiation of pulsed n/γ mixing radiation fields is of great importance to the inertial confinement fusion experiment, magnetic fusion experiment and other pulsed n/γ mixing radiation fields.[1–5] It offers a way to explore the reaction process. $LaBr_3$(Ce) scintillators,[6] with excellent scintillation time, high light yields and resilience to neutron damage, have been employed in the measurements of gamma-ray spectroscopy and gamma-ray flux in pulsed n/γ mixing radiation fields.[7–9]

In pulsed n/γ mixing radiation fields, gamma rays and neutrons are always mixed. Besides the calibration of the scintillator response to gamma rays, the calibration of the scintillator response to neutron irradiation also affects the accuracy of the absolute measurement of gamma radiation. Therefore, a detailed study of the scintillator response to neutron irradiation is required for the design of suitable lines of sight and neutron filters, and to aid in the interpretation of the measurements.[8]

Over the last few years, various studies focusing on the neutron response of the $LaBr_3$(Ce) scintillator have been performed. Cazzaniga *et al.*[8–10] measured the response of $LaBr_3$(Ce) scintillators to 2.5 MeV neutrons and 14 MeV neutrons at the Frascati Neutron Generator, respectively. The main contributors to the measured neutron responses were studied. Lu *et al.*[11] studied the relative sensitivities of a $LaBr_3$(Ce) scintillation detector to 1.25 MeV γ-rays, and 2.5 MeV and 14 MeV neutrons. Ebran *et al.*[12] reported measurement of the neutron detection efficiency in a $LaBr_3$(Ce) scintillation detector in the energy range 0.1–2 MeV. Lu *et al.*[13] studied the resistance to neutron irradiation of a $LaBr_3$(Ce) scintillator. Kiener *et al.*[14] determined neutron-interaction yields in a 1.5-in. cylindrical $LaBr_3$(Ce) crystal in the energy range 2.8–11.6 MeV. The energy spectra of the $LaBr_3$(Ce) resulting from fast neutron interactions were obtained at four different neutron energies. Tain *et al.*[15] studied the neutron sensitivity of a Φ1.5 in.$\times$1.5 in. $LaBr_3$(Ce) scintillation detector using quasi-monoenergetic neutron beams at five different energies in the range from 40 keV to 2.5 MeV. Taggart *et al.*[16] studied the response of a $LaBr_3$(Ce) scintillator to the fast neutrons produced by an Am–Be source. Neutron-induced charged-particle reactions were observed in the $LaBr_3$(Ce) scintillator. However, there are some disadvantages in the above studies. First, there are few available energy points. In addition, the above studies mainly focused on the pulse height spectrum resulting from the neutron interactions and neutron detection efficiency. Only one paper[11] reported the neutron sensitivity of $LaBr_3$(Ce) scintillation in current mode,[17] which was one of the key parameters of the

†Corresponding author. E-mail: yilt2008@163.com

© 2023 Chinese Physical Society and IOP Publishing Ltd

detector for neutron flux measurement in the pulsed n/γ mixing radiation fields. But the neutron energies in the pulsed n/γ mixing radiation fields are continuous; the neutron sensitivity curve is thus needed. One solution is to simulate the neutron sensitivity curve.

However, the luminescence process of inorganic scintillators is very complicated and it primarily results from the energy deposition of secondary charged particles. The secondary charged particles produced by neutrons for $LaBr_3$(Ce) scintillation were electrons, alpha particles, protons and deuterium particles, but there were no luminescence data for these secondary charged particles. The neutron sensitivity curve of the $LaBr_3$(Ce) scintillator cannot be accurately simulated. Therefore, experimental study on the neutron sensitivity of the $LaBr_3$(Ce) scintillator is crucial for its use in the absolute gamma measurement of pulsed radiation fields. This is also crucial for other inorganic scintillators.

The China Spallation Neutron Source (CSNS) produces neutrons by slamming 1.6 GeV protons onto a tungsten target with a 25 Hz repetition frequency. An associated Back-n white neutron source of CSNS was exploited for nuclear data measurement. It has a series of precise energy points and a wide energy range, which provides applicable conditions for experimental study on the neutron sensitivity of a scintillator.[18–20] The CSNS accelerator has two modes of operation, double-bunch and single-bunch modes, with the former mode being the primary mode. In this mode, the second proton bunch arrives approximately 410 ns after the first bunch, and the neutron intensity is double that of the single-bunch mode. However, because of time-of-flight dispersion, the energy resolution is lower than that in the single-bunch mode. Therefore, it may influence the measured results of the neutron sensitivity experiment.

In this work, a scintillator detector consisting of a $LaBr_3$(Ce) scintillator and a photomultiplier tube (PMT) was used to study the neutron sensitivities of the $LaBr_3$(Ce) scintillator at the CSNS Back-n white neutron source end station 2 in double-bunch and single-bunch operation modes, respectively. Under double-bunch and single-bunch operation modes, the relative neutron sensitivity curves of the $LaBr_3$(Ce) scintillator in the energy regions of 1–20 MeV and 0.5–20 MeV were obtained for the first time. The results indicated that the two curves were nearly identical in the energy range of 1–20 MeV. But the single-bunch experiment's neutron sensitivity curve has a lower minimum measurable energy and a smaller relative neutron sensitivity uncertainty than the double-bunch experiment.

2. Experimental setup

The experiments were performed at the CSNS Back-n white neutron source end station 2 (ES2#)[18] under double-bunch and single-bunch operation mode, respectively, as shown in Fig. 1(a). The sizes of the neutron shutter, collimator 1 and collimator 2 during the two experiments are shown in Table 1. The beam spot sizes of ES#2 were Φ30 mm and Φ42 mm, respectively. The operating powers were 50 kW and 40 kW, respectively. The distances from the tungsten target to the front end of the scintillation detector were 74.70 m and 74.53 m, respectively.

Table 1. Neutron beam conditions.

Operating mode	Neutron shutter (mm)	Collimator 1 (mm)	Collimator 2 (mm)	Beam spot size (mm)	Operating power (kW)	Neutron flux (cm^{-2}/pulse)
Double-bunch	Φ12	Φ15	Φ40	Φ30	50	1.6×10^4
Single-bunch	Φ50	Φ50	Φ40	Φ42	40	2.2×10^5

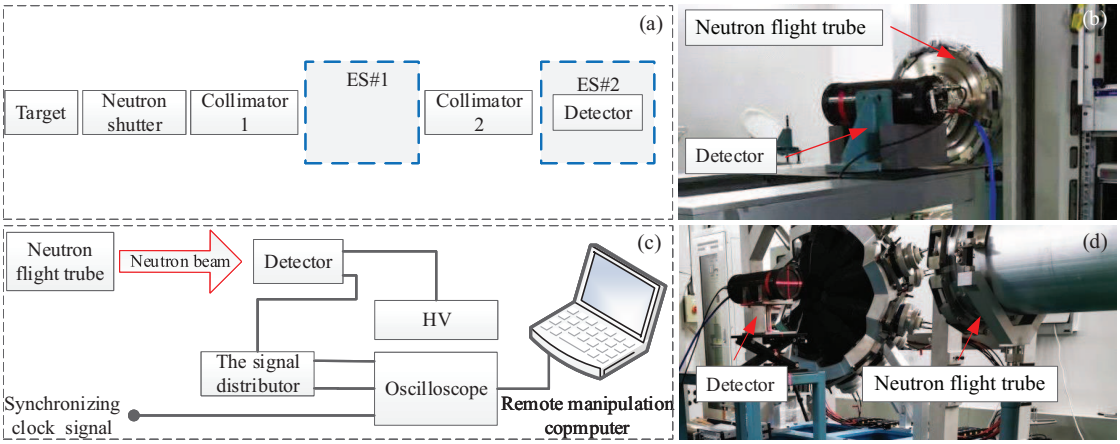


Fig. 1. (a) A schematic diagram of the detector installation position. (b) The experimental setup of the double-bunch experiment. (c) A schematic diagram of the experimental arrangement. (d) The experimental setup of the single-bunch experiment.

As shown in Fig. 1(c), the data record mode was the same in the two experiments. The detector signal was divided into two channels and recorded by an oscilloscope (Agilent, DSOX4154A). One channel was used to trigger the oscilloscope and record the gamma flash signals,[21] which were mainly generated in the detector by the γ-rays produced during the spallation process. Except for trigging the oscilloscope, the gamma flash signal was used to measure the neuron flight time. The other channel was used to record the neutron signal. The synchronizing clock signal was used to monitor the state of the neutron beam. In the double-bunch experiment, the detector was installed in a side view. As shown in Fig. 1(b), the axis of the detector was perpendicular to the direction of the neutron beam. In the single-bunch experiment, the detector was installed in a front view. As shown in Fig. 1(d), the axis of the detector was parallel to the direction of the neutron beam.

A schematic diagram of the scintillation detector is shown in Fig. 2. It consisted of PMT (Hamamatsu, RC392) and Φ80 mm$\times$20 mm $LaBr_3$(Ce) (5%) scintillation, as shown in Figs. 2(c) and 2(d). They were sealed in a carbon steel sleeve to shield them from light and electromagnetic interference. The thickness of the carbon steel in front of the scintillator was 1 mm and the carbon steel surrounding the scintillator and PMT was 2 mm. The scintillator was fixed in the detector by a group of polytetrafluoroethylene fixed collars. During the double-bunch experiment, the scintillator and PMT were coupled by silicone grease. The distance from the detector's front window to the center of the scintillator was 40 mm, as shown in Fig. 1(a). During the single-bunch experiment, the scintillator was fixed to the detector front window to reduce the signal intensity, as shown in Fig. 1(b). The distance from the PMT photocathode to the center of the scintillator was 40 mm.

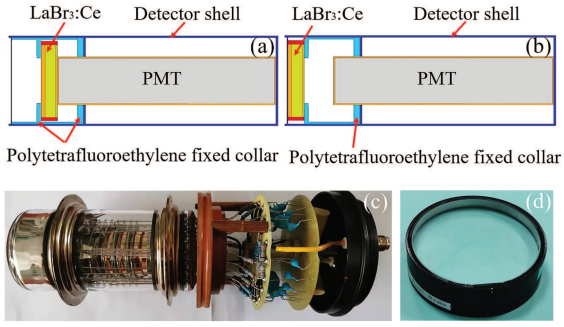


Fig. 2. (a) A schematic diagram of the scintillation detector in the double-bunch experiment. (b) A schematic diagram of the scintillation detector in the single-bunch experiment. (c) CR392 PMT. (d) $LaBr_3$(Ce) scintillation.

3. Results and discussion

3.1. Background signal analysis

Because of the high gamma and neutron sensitivities of the $LaBr_3$(Ce) scintillator and the accompanying gamma background in the neutron radiation field, it is necessary to first measure the background signals to obtain an accurate neutron response signal from the $LaBr_3$(Ce) scintillator. The primary background signals for this experiment were the scattered neutrons and gamma rays produced by structures of the scintillation detector, environmental background radiation and PMT photocathode response signals.

Geant4,[22,23] a Monte Carlo particle transport code, was utilized to simulate the signal-to-noise ratios of scattered neutrons and scattered gamma rays produced by the detector shell, fixed collar and other structures of the scintillation detector. High-precision neutron models and cross sections were used to describe elastic scattering and inelastic reactions for neutrons with energies below 20 MeV. The default physics list FTFP BERT was used for neutrons with energies exceeding 20 MeV. The G4EmStandardPhysics_option4 physics list was used to describe the electromagnetic processes of γ, e^-, e^+ and heavy charged particles. As shown in Fig. 3, the signal-to-noise ratios of secondary neutrons and gamma rays in the double-bunch experiment were greater than 15 and 75, respectively. The signal-to-noise ratios of secondary neutrons and gamma rays in the single-bunch experiment were greater than 40 and 143, respectively. The results suggested a favorable measurement environment.

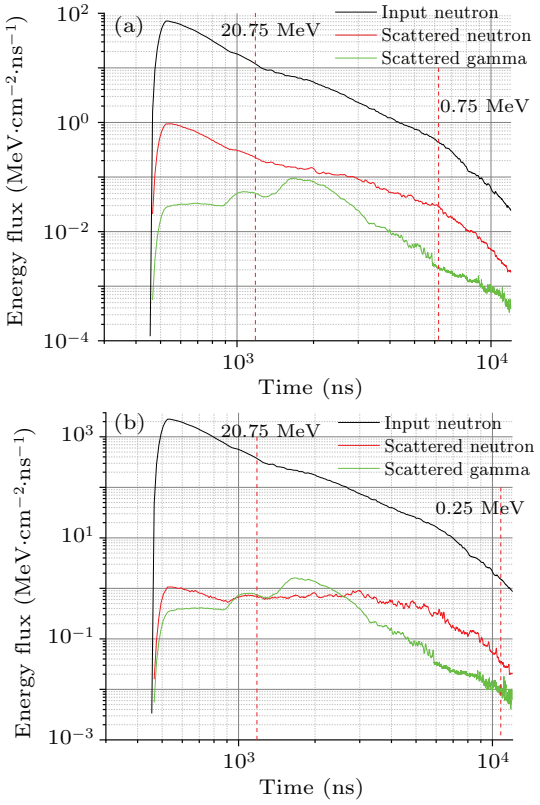


Fig. 3. The energy flux of the scattered neutrons and gamma rays produced by structures of the scintillation detector. (a) Double-bunch experiment. (b) Single-bunch experiment.

The environmental background radiation was measured by placing the detector 10 cm away from the neutron beam. The results indicate that the oscilloscope contained only a

baseline. This suggests that environmental background radiation can be ignored in this experiment.

To measure the intensity of the PMT photocathode response signal, a detector without a scintillator was installed with a frontal view in the single-bunch experiment. As depicted in Fig. 4, the maximum neutron signal amplitude of the measured PMT photocathode response signal was 1.8 mV. Meanwhile, the maximum net neutron signal amplitude of the single-bunch experiment was 634 mV. The maximum PMT photocathode response signal amplitude was significantly less than the maximum net neutron signal amplitude. Because the neutron flux in the double-bunch experiment was only 1/20 of that of the single-bunch experiment, the maximum neutron signal amplitude of the measured PMT photocathode response signal was less than 0.1 mV in the double-bunch experiment. But the maximum net neutron signal amplitude of the double-bunch experiment was 200 mV. The maximum amplitude of the PMT photocathode response signal was also considerably smaller than that of the neutron signal in the double-bunch experiment. The above results imply that the PMT photocathode response signal in this experiment can be ignored. The preceding results demonstrated that the experiment's background signals can be ignored.

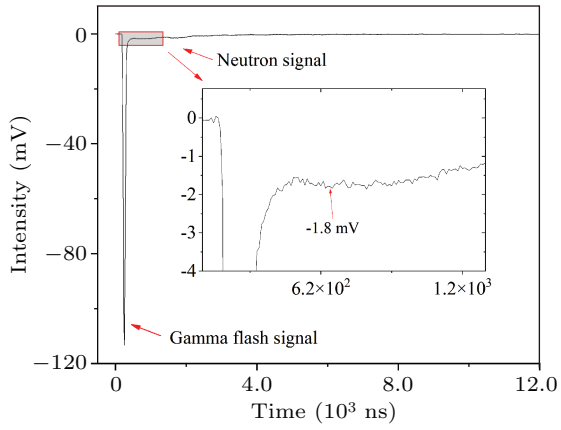


Fig. 4. The measured PMT photocathode response signal.

3.2. Spectrum unfolding calculation

In double-bunch operation mode, the rapid cycling synchrotron accumulates two proton bunches separated by approximately 410 ns.[19] The two proton bunches in a single pulse have a substantial effect on the neutron pulse. The measured signal can therefore be considered the superposition of two identical signals, separated by approximately 410 ns. It can be expressed using the equation below:

$$F(t) = f_1(t) + f_2(t), \tag{1}$$

$$f_2(t) = w_2 f_1(t - \Delta t), \tag{2}$$

where $F(t)$ is the measured signal, $f_1(t)$ and $f_2(t)$ are the signals of bunch 1 and bunch 2, respectively, Δt is the time lag of the two bunches, and w_2 is the intensity ratio of bunch 2 signal to bunch 1 signal.

As shown in Fig. 5, two gamma flash signals were detected in the measured signal. Using Eqs. (1) and (2), signal bunches 1 and 2 were calculated. The time lag and intensity ratio were 409 ns and 0.998, respectively. As the signals from bunches 1 and 2 were nearly identical, the signal from bunch 2 was used to calculate the neutron sensitivity.

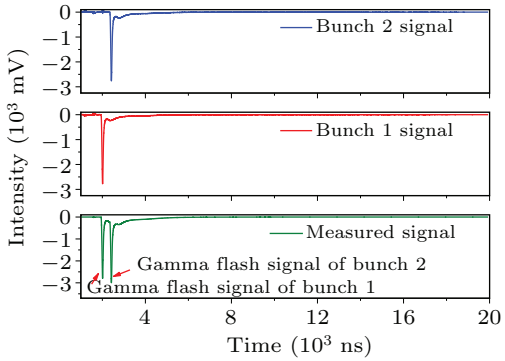


Fig. 5. The measured signal of $LaBr_3(Ce)$ in double-bunch operation mode.

3.3. Relative neutron sensitivity analysis

In this experiment, the neutron energy was determined using the time-of-flight method. The peak moment of a gamma flash signal was used to measure the time-of-flight of the neutron. As 40 mm was considerably shorter than 74.53 m, it was ignored when measuring the neutron's flight time. For a precise time-of-flight spectrum, the Monte Carlo method was used. Chen *et al.*[21] obtained the energy spectrum of the end station 2, and the full width half maximum (FWHM) of the source was 50 ns.[24] The calculated neutron time-of-flight spectrum produced by a bunch is shown in Fig. 6.

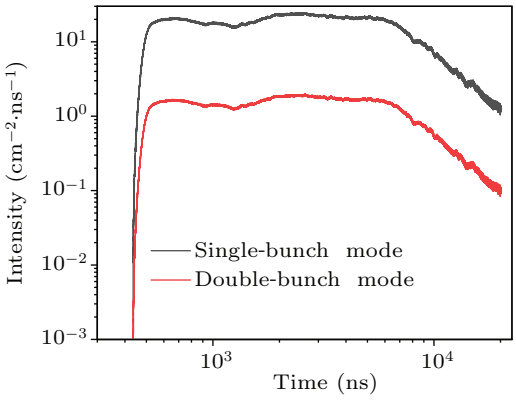


Fig. 6. The neutron time-of-flight spectrum produced by a bunch at the detector position.

As shown in Fig. 7, the amplitude of the gamma flash signal was significantly greater than the neutron signal. The gamma flash's trailing peak overlapped with the neutron signal. Since the gamma flash and neutron were generated simultaneously,[21] the gamma flash signal could not be detected independently. Before the trailing fall to the baseline,

the neutron signal had appeared. The complete gamma flash peak and net neutron signal cannot be determined through experimentation. To obtain the net neutron signal, the trailing of the gamma flash peak should be subtracted from the measured neutron signal. The following equation was used to fit the gamma flash peak, which was an empirical formula:

$$P(t) = \sum_{i=1}^{3} \left(P_{0i} + A_i \cdot \exp\left(-\exp\left(-z_i\right) - z_i + 1\right)\right), \quad (3)$$

$$Z_i = (t - tc_i)/w_i. \quad (4)$$

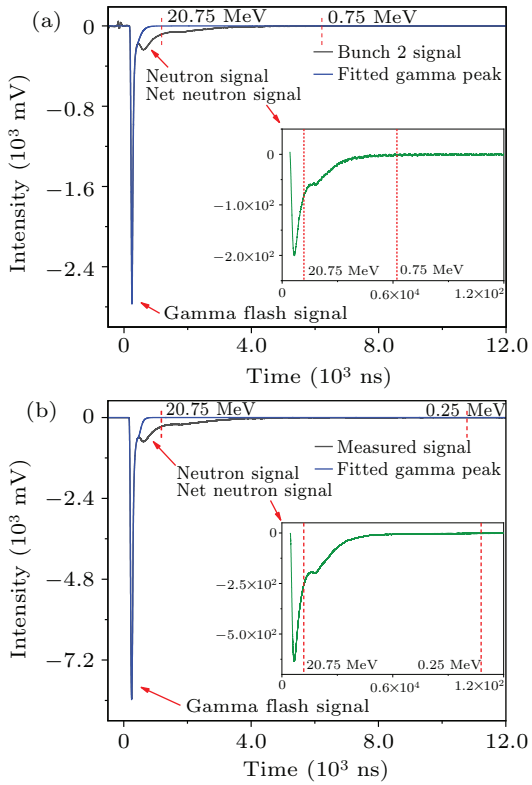


Fig. 7. The measured signals, fitted gamma flash peaks and net neutron signals. (a) Double-bunch experiment. (b) Single-bunch experiment.

The measured signals and fitted gamma flash peaks of the $LaBr_3$(Ce) scintillators are shown in Fig. 7. The maximum net neutron signal amplitudes of the double-bunch and single-bunch experiments were 200 mV and 634 mV, respectively. The neutron signal shapes of the two experiments were almost the same. Because the bunch 2 signal was calculated, it was not as smooth as the measured signal of the single-bunch experiment and had a higher baseline. The net signal intensity of the double-bunch experiment was too small to calculate the neutron sensitivity when the neutron energy was below 0.75 MeV. Meanwhile, that of the single-bunch experiment result was less than 0.25 MeV.

To calculate the neutron sensitivity,[18] the net neutron signal wave was divided into multiple regions. The region's range was determined by the energy interval of the neutron sensitivity curve. Here, the energy interval was 0.5 MeV in the range of 1–5 MeV, 1 MeV in the range of 5–10 MeV and 1.5 MeV in the range of 11–20 MeV. The neutron sensitivity was calculated using

$$S(E_i) = \frac{\sum (V_j \cdot \Delta t/R)}{N_i}, \quad (5)$$

where E_i is the central energy of region i, V_j is the amplitude of sampling site j of the neutron response signal, N_i is the total neutron counts in region i, Δt (0.4 ns) is the sampling interval of the oscilloscope and R (50 Ω) is the impedance of the detector.

In addition to calculating the neutron sensitivity uncertainty, the neutron energy uncertainty was calculated, as the neutron source was not a delta source. Using the following equation, the neutron energy uncertainty and neutron sensitivity uncertainty were calculated:

$$u_C = \sqrt{\sum_{j=1}^{n} u_j^2}. \quad (6)$$

The components of u_j are listed in Table 1.

Table 2. The components of u_j.

j	u_j neutron energy uncertainty	u_j neutron sensitivity uncertainty
1	The pulse width of the neutron source	The statistical fluctuation of neutron counts in region i
2	The uncertainties of the fitted gamma flash peak position	The uncertainties of the net neutron signal amplitude in region i
3	The energy interval of the neutron sensitivity curve	The uncertainties of the fitted gamma flash signal
4	The sampling interval of the oscilloscope	–
5	The time response of the detector	–

Since the neutron flux curve meeting the requirements of the absolute sensitivity calibration experiment cannot be measured, the relative neutron sensitivity curves were calculated in this experiment. Using some special energy points, such as 2.5 MeV and 14.1 MeV, the absolute neutron sensitivity curve of the $LaBr_3$(Ce) can be calibrated. Using the absolute neutron sensitivity curve, the signal amplitude of the detector caused by scattered neutrons and secondary neutrons can be calculated. These data are the basic data of the effectiveness evaluation of the neutron collimator and filter, and can be used to analyze the measured data.

By normalizing the neutron sensitivity to the 14 MeV neutron, the relative neutron sensitivity curves of the $LaBr_3$(Ce) scintillator in the energy regions of 1–20 MeV and

0.5–20 MeV were obtained for the first time using the double-bunch and single-bunch operation modes. The experimental method used herein has been verified in our previous study.[25] As shown in Fig. 8, the two curves were nearly identical in the energy range of 1–20 MeV. Since a spectrum unfolding calculation was performed on the double-bunch experimental results, the FWHM of the neutron signal baseline was larger than that of the single-bunch experiment and the net neutron signal of the double-bunch experiment was rougher than that of the single-bunch experiment. The double-bunch experiment produced a neutron sensitivity curve with a minimum detectable energy of 1 MeV. In contrast, the value for the single-bunch experiment was 0.5 MeV.

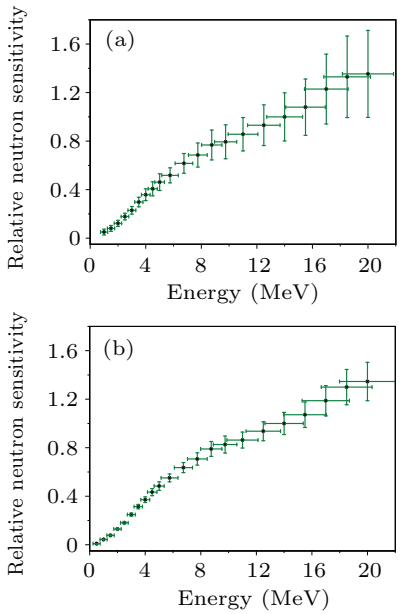


Fig. 8. The relative neutron sensitivity curves of the $LaBr_3(Ce)$ scintillator. (a) Double-bunch experiment. (b) Single-bunch experiment.

The maximum and minimum expanded uncertainties ($k = 2$)[26] of the relative neutron sensitivity of the double-bunch experiment were 47.4% and 13.2% at 1 MeV and 3.5 MeV, respectively. The maximum and minimum expanded uncertainties ($k = 2$) of the relative neutron sensitivities of the single-bunch experiment were 47.4% and 11.8% at 0.5 MeV and 20 MeV, respectively. The spectrum unfolding calculation introduced computational noise into the calculated results, and the calculated neutron response signal of the double-bunch experiment was not as smooth as the measured neutron response signal of the single-bunch experiment. The uncertainties of the fitted gamma flash signal in the double-bunch experiment were significantly greater than in the single-bunch experiment. Thus, the relative neutron sensitivity uncertainties of the double-bunch experiment were greater than those of the single-bunch experiment.

The preceding results indicated that the single-bunch experiment's neutron sensitivity curve has a lower minimum measurable energy than the double-bunch experiment. In the energy range of 1–20 MeV, there is little difference between the single-bunch and double-bunch experimental results of the $LaBr_3(Ce)$ scintillator.

4. Conclusions

In this paper, the neutron sensitivities of the scintillation detector were investigated at the CSNS Back-n white neutron source end station 2. Under double-bunch and single-bunch operation modes, the relative neutron sensitivity curves of the $LaBr_3(Ce)$ scintillator in the energy regions of 1–20 MeV and 0.5–20 MeV were obtained for the first time. In the energy range of 1–20 MeV, the two curves were nearly identical. However, the relative neutron sensitivity uncertainties of the double-bunch experiment were higher than those of the single-bunch experiment.

The single-bunch experiment's neutron sensitivity curve has a lower minimum measurable energy than the double-bunch experiment. The higher the neutron response signal intensity, the lower the minimum measurable energy of the neutron sensitivity curve. Above the minimum measurable energy of the double-bunch experiment, there is little difference between the measured relative neutron sensitivity curves of the single-bunch and double-bunch experiments of the $LaBr_3(Ce)$ scintillator and those of other scintillators with a similar neutron response signal intensity.

Acknowledgements

Project supported by the National Natural Science Foundation of China (Grant No. 11905196). The authors would like to thank their colleagues from CSNS for their support.

References

[1] Merrill F E, Danly C R, Fittinghoff D N, Grim G P, Guler N, Volegov P L and Wilde C H 2016 *J. Phys.: Conf. Ser.* **688** 012064
[2] Kiptily V G, Cecil F E and Medle S S 2006 *Plasma Physics and Controlled Fusion* **48** R59
[3] Chugunov I N, Shevelev A E, Gin D B, Kiptily V G, Gorini G, Nocente M, Tardocchi M, Doinikov D N, Naidenov V O and Khilkevitch E M 2011 *Nucl. Fusion* **51** 083010
[4] Ouyang X 2008 *Strategic Study of CAE* **10** 44 (in Chinese)
[5] Xing B, Wang F and Fan J 2016 *Fanghua Yanjiu* **1** 33 (in Chinese)
[6] Bizarri G and Dorenbos P 2007 *Phys. Rev. B* **75** 184302
[7] Tardocchi M, Nocente M and Gorini G 2013 *Plasma Physics and Controlled Fusion* **55** 074014
[8] Cazzaniga C, Nocente M, Tardocchi M, Rebai M, Pillon M, Camera F, Giaz A, Pellegri L and Gorini G 2015 *Nucl. Instrum. Meth. Phys. Res. A* **778** 20
[9] Cazzaniga C, Nocente M, Tardocchi M, Croci G, Giacomelli L, Angelone M, Pillon M, Villari S, Weller A, Petrizzi L and Gorini G 2013 *Rev. Sci. Instrum.* **84** 123505
[10] Cazzaniga C, Giacomelli L, Grosso G, Nocente M, Tardocchi M, Gorini G, Weller A and ASDEX Upgrade team 2013 *Nucl. Instrum. Meth. Phys. Res. A* **732** 384
[11] Lu Y, Song Z, Tan X, Zhao X, Zhang Z, Li G and Zhang K 2014 *Atomic Energy Science and Technology* **48** 158 (in Chinese)

[12] Ebran A, Roig O, Méot V and Delaune O 2014 *Nucl. Instrum. Meth. Phys. Res. A* **768** 124
[13] Lu Y, Song Z, Li G, Tian J, Zhao X and Zhang K 2015 *Chin. Phys. C* **39** 106003
[14] Kiener J, Tatischeff V, Deloncle I, Séréville N, Laurent P, Blondel C, Chabot M, Chipaux R, Coc A, Dubos S, Gostoji A, Goutev N, Hamadache C, Hammache F, Horeau B, Limousin O, Ouichaoui S, Prévot G, Rodríguez-Gasén R and Yavahchova M S 2015 *Nucl. Instrum. Meth. Phys. Res. A* **798** 152
[15] Tain J L, Agramunt J, Algora A, Aprahamian A, Cano-Ott D, Fraile L M, Guerrero C, Jordan M D, Mach H, Martinez T, Mendoza E, Mosconi M and Nolte R 2015 *Nucl. Instrum. Meth. Phys. Res. A* **774** 17
[16] Taggart M P and Henderson J 2020 *Nucl. Instrum. Meth. Phys. Res. A* **975** 164201
[17] Zhang Q, Wang Q, Xie Z and Niu S 2003 *Nucl. Instrum. Meth. Phys. Res. A.* **496** 146
[18] An Q, Bai H Y, Bao J, *et al.* 2017 *JINST* **12** P07022
[19] Tang J, An Q, Bai J, *et al.* 2021 *Nucl. Sci. Tech.* **32** 11
[20] Yu Q Z, Liang T J, Yin W, Yan Q W, Jia X J and Wang F W 2009 *Chin. Phys. B* **18** 3815
[21] Chen Y H, Luan G Y, Bao J, Jing H and Zhu P 2019 *Eur. Phys. J. A* **55** 115
[22] Agostinelli S, Allison S, Amako K, *et al.* 2003 *Nucl. Instrum. Meth. Phys. Res. A* **506** 250
[23] Allison J, Amako K, Apostolakis J, *et al.* 2006 *IEEE Trans. Nucl. Sci.* **53** 270
[24] Zhang L 2018 *Study and physical design of white neutron beamlines at CSNS* (Ph. D. Dissertation) (Hefei: University of Science and Technology of China) (in Chinese)
[25] Yi L, Liu J, Tang D, Wang D, Li Z, Hu M, Yi H and Zhang F 2023 *Nucl. Instrum. Meth. Phys. Res. A* **1046** 167698
[26] Li S A 2005 *Industrial Measurement* **15** 35 (in Chinese)